Available online at www.sciencedirect.com
ScienceDirect
Sensors and Actuators A 145–146 (2008) 87–93
SENSORS AND ACTUATORS A PHYSICAL
www.elsevier.com/locate/sna

Microfabricated VHF acoustic crystals and waveguides

Roy H. Olsson III [a,*], Ihab F. El-Kady [a,b], Mehmet F. Su [b], Melanie R. Tuck [a], James G. Fleming [a]

[a] *Advanced MEMS Department, Sandia National Laboratories, Albuquerque, NM, USA*
[b] *Electrical and Computer Engineering Department, University of New Mexico, Albuquerque, NM, USA*

Received 29 June 2007; received in revised form 9 October 2007; accepted 21 October 2007
Available online 12 November 2007

Abstract

Microfabricated acoustic crystals have been designed and experimentally verified. The acoustic crystals are realized by including tungsten (W) scatterers in a SiO_2 matrix. Wide frequency ranges where acoustic waves are forbidden to exist (acoustic bandgaps, ABG) are formed due to the large acoustic impedance and mass density mismatch between W and SiO_2. The acoustic crystal structures are fabricated in a 7-mask process that features integrated aluminum nitride piezoelectric couplers for interrogating the devices. Acoustic crystals in a square lattice have been measured at 67 MHz with greater than 30 dB of acoustic rejection and bandwidths exceeding 25% of the midgap. Single and multimode acoustic waveguides have been realized by defecting the acoustic crystals through removal of a subset of the W scatterers. These waveguides achieve relative transmission of up to 100% for the propagating modes.

Keywords: Acoustic bandgap; Acoustic crystal; Aluminum nitride; Phononic bandgap; Phononic crystal; Waveguide

1. Introduction

Acoustic crystal or acoustic bandgap (ABG) is the acoustic wave equivalent of photonic crystal or photonic bandgap (PBG), where a range of acoustic frequencies are forbidden to exist in a structured material. ABGs are realized by including periodic scatterers in a matrix that propagates an acoustic wave. Micro-ABGs are useful for acoustic isolation of devices such as RF resonators and gyroscopes. The bandwidth of an ABG isolator, $\Delta\omega$, can exceed $0.5\omega_g$ [1], where ω_g is the center frequency of the ABG. This wide bandwidth distinguishes ABG acoustic isolators from previously developed one-dimensional quarter-wave acoustic reflectors [2]. Furthermore, by strategically locating defects in the ABG through removal or distortion of the scatterers, micro-acoustic waveguides, focusing, sensors, high-Q cavities, and advanced acoustic signal processors can be realized. These devices have applications in communications, ultrasound, sensing and non-destructive testing. ABGs also provide precise control of phonon propagation and distribution, a useful tool for studying phonons.

Most of the prior experimental ABG work has been limited to large, hand-assembled structures at frequencies below 1 MHz, where the ABG matrix material was either water or epoxy [3–6]. Investigation of higher frequency ABGs in solid, low-loss materials has recently been reported for surface acoustic waves (SAW) where ABGs have been demonstrated at 200 MHz by etching air hole scatterers in lithium niobate [7] and Si [8]. Microfabricated ABGs realized in a suspended slab were first reported in Ref. [9] and have several significant advantages over SAW approaches. Most importantly, these slab devices can be placed in vacuum and are isolated from the substrate, completely confining the acoustic energy inside a two-dimensional ABG. In SAW ABGs, energy can radiate into the substrate [7], introducing loss in ABG based devices such as cavities and waveguides. Other advantages of the microfabricated ABGs reported here are small size, post-CMOS integration, and the ability to realize cermet [4–6,9], rather than network [7,8], topology acoustic crystals which achieve higher acoustic attenuation over a wider frequency range [10]. The realization of acoustic bandgap based devices such as cavities and waveguides has also been limited to hand-assembled, bulk acoustic wave structures operating at frequencies below 1 MHz [3,11].

In this paper, we report microfabrictaed acoustic crystal slabs and acoustic bandgap based waveguides that scale pre-

* Corresponding author. Tel.: +1 505 284 6375; fax: +1 505 844 2081.
E-mail address: rholsso@sandia.gov (R.H. Olsson III).

0924-4247/$ – see front matter © 2007 Elsevier B.V. All rights reserved.
doi:10.1016/j.sna.2007.10.081

vious macroscale ABG work to the microscale and to VHF frequencies. The micro-ABGs, realized by including high-acoustic impedance, high-density W scatterers in a low-acoustic impedance, low-density SiO_2 background matrix, are fabricated in a 7-level process that is post-CMOS compatible and integrates thin film aluminum nitride (AlN) piezoelectric couplers for electronic interrogation of the ABG devices. Micro-ABG slabs have been developed and characterized at 67 MHz corresponding to a lattice constant of 45 μm. These acoustic crystals achieve greater than 30 dB of acoustic rejection inside the gap region and gap bandwidths exceeding 25% of the gap center frequency. W1 and W3 waveguides, corresponding to removal of one and three rows of W scatterers from the acoustic crystal slab, have been demonstrated, achieving 100% relative transmission for some propagating modes.

2. Acoustic bandgap device design and operation

To produce an acoustic bandgap spanning a wide frequency range with large acoustic isolation several important criteria should be considered. First, a cermet topology of unconnected high-acoustic impedance inclusions in a low-acoustic impedance matrix material with as high an acoustic impedance contrast as possible between the inclusions and the matrix should be used [10]. Using a cermet topology to achieve wide gaps is opposite to photonic crystals where a network topology (the scattering inclusions are connected) is preferred [10]. The acoustic impedance of a material is:

$$Z_m = c_m \rho_m, \quad (1)$$

where c_m is the acoustic velocity and ρ_m is the density. Etching large hole inclusions in a solid matrix [7,8] creates a network topology of low-acoustic impedance scatterers in a high-acoustic impedance matrix. This results in narrower bandgaps and lower isolation than placing a high impedance scatterer in the same matrix material. Second, the velocity of the matrix and scattering material should be sufficiently mismatched, with $c_{matrix} > c_{inclusion}$, to enable the simultaneous realization of both the Bragg and Mie resonance conditions [12] while maintaining a reasonable volume filling fraction (*r/a* in Fig. 1) of the high-acoustic impedance inclusions in the matrix. Too low a filling fraction allows transmission through the matrix material around the scatterers. On the other hand, if the filling fraction becomes too high, hopping between the scatterers leads to acoustic transmission. Finite difference time domain (FDTD) simulations indicate the optimal ratio, *r/a*, for the ABGs reported here to be 0.32. Since the velocity of the scattering inclusion should be lower than that of the matrix while the acoustic impedance of the inclusion should be many times higher than that of the matrix, from (1), a large density mismatch is needed between the inclusions and the matrix with $\rho_{inclusion} \gg \rho_{matrix}$ [12]. Other material considerations include material damping and silicon CMOS compatibility.

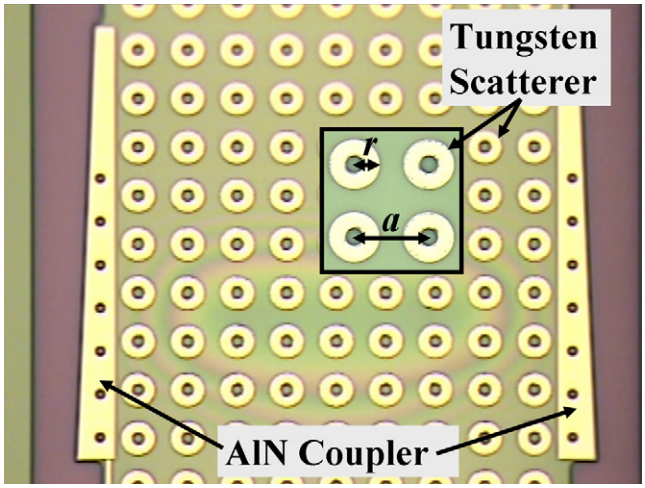

Fig. 1. Micro-ABG slab with integrated AlN electro-acoustic couplers. The ABG is realized by including W scatterers in an oxide matrix. Acoustic frequencies within the gap cannot pass between the AlN couplers. Inset shows close up image of the W scatterers and release holes. The lattice constant, *a*, is 45 μm and *r* is 14.4 μm, yielding a volume filling fraction of 0.32. The release holes in the center of the W inclusions have a radius of 5 μm.

Tables 1 and 2 summarize the acoustic properties of potential inclusion and matrix materials respectfully. Tungsten is an excellent choice for the scattering inclusion because of its high acoustic impedance, 89 MΩ, and mass density, 19,000 kg/m^3. Tungsten also has low material damping ($Q > 10^5$ at 300 K [13]) and is widely used in CMOS contact structures. The choice of a matrix material requires more consideration. Polymers such as SU-8 will achieve very high acoustic impedance mismatch with W. The material damping, however, is high and the acoustic velocity is low, resulting in smaller structures that are more difficult to fabricate for a given frequency. Alternatively, a material such as Si, either single crystal or polycrystalline, can be used. Quality factors exceeding 10^5 [15] have been achieved in microfabricated Si resonators and the acoustic velocity is high. Of low loss, high velocity MEMS materials, SiO_2 has the largest impedance mismatch with W and has been chosen for this work to achieve the widest possible gaps.

A 67 MHz microfabricated W/SiO_2 square lattice ABG slab is pictured in Fig. 1. Acoustic energy is coupled into and out of the device in the form of longitudinal acoustic waves using electrically driven AlN piezoelectric couplers. The couplers are

Table 1
Acoustic properties of potential μABG inclusion materials

Inclusion material	Mass density (kg/m^3)	Acoustic velocity (km/s)	Acoustic impedance (MΩ)	Previously reported quality factor
Mo	10,300	5.7	59	416,000 [13]
Pt	21,440	2.8	60	8,500 [14]
PolyDiamond	3,500	18.5	65	12,000 [15]
W	19,300	4.6	89	238,000 [13]